Magneto-Rayleigh–Taylor instability in compressible Z-pinch liner plasmas*

Xue Yang(杨学)[1,2], De-Long Xiao(肖德龙)[1,†], Ning Ding(丁宁)[1], and Jie Liu(刘杰)[1,3]

[1] *Institute of Applied Physics and Computational Mathematics, Beijing* 100088, *China*
[2] *Graduate School, China Academy of Engineering Physics, Beijing* 100088, *China*
[3] *HEDPS, CAPT, and CICIFSA MoE, Peking University, Beijing* 100871, *China*

(Received 17 January 2017; revised manuscript received 7 April 2017; published online 6 June 2017)

In this paper, the characteristics of magneto-Rayleigh–Taylor (MRT) instability of liner plasmas in MagLIF is theoretically investigated. A three-region slab model, based on ideal MHD equations, is used to derive the dispersion relation of MRT instability. The effect of compressibility on the development of MRT instability is specially examined. It is shown that the growth rate of MRT instability in compressible condition is generally lower than that in incompressible condition in the presence of magnetic field. In the case of zero magnetic field, the growth rate in compressible assumption is approximately the same as that in incompressible assumption. Generally, MRT instability in (x,y) plane can be remarkably mitigated due to the presence of magnetic field especially for short-wavelength perturbations. Perturbations may be nearly completely mitigated when the magnetic field is increased to over 1000 T during liner implosions. The feedthrough of MRT instability in liner outer surface on inner surface is also discussed.

Keywords: magneto-Rayleigh–Taylor (MRT) instability, magnetized liner inertial fusion (MagLIF), Z-pinch, compressibility

PACS: 52.57.Fg, 52.55.Tn, 52.58.Lq **DOI:** 10.1088/1674-1056/26/7/075202

1. Introduction

In the magnetized liner inertial fusion (MagLIF), which is proposed by the Sandia National Laboratories, the preheated and premagnetized fuel is compressed and confined by a cylindrical Z-pinch liner.[1] In recent integrated MagLIF experiments on the Z machine, over 10^{12} fusion neutrons were generated, which shows great potential of MagLIF in driving inertial confinement fusion.[2] The most important physical problem in MagLIF is the magneto-Rayleigh–Taylor (MRT) instability, which is inherent to Z-pinch implosions.[2–8] The development of MRT instability may cause the disruption of liner implosions and the severe mixing of fuel with the liner, and then limit the fuel to reach ignition condition.[1]

MRT instability in magnetohydrodynamics (MHD) was firstly studied by Chandrasekhar in 1961.[9] Harris studied the MRT instability of an infinitesimal thickness cylindrical shell in a magnetic field.[10] The gradient effects for a particular exponential profile in density and magnetic field were also studied.[11] Zhang *et al*. discussed the effect of equilibrium shear flow on enhancing MRT instability because of its coupling with a Kelvin–Helmholtz-type instability.[12] Bud'ko *et al*. studied the stability of dynamic Z pinches and theta pinches and found that in the case of a dynamic Z-pinch, the growth rate is much higher than that in the equilibrium case in 1989.[13] Bellan obtained the dispersion relation and analyzed the MRT instability in an incompressible magnetized plasma.[14] These studies were performed by using two-region model with vacuum and infinite plasmas. For MagLIF, Lau *et al*. firstly developed a three-region model, which consists of vacuum, liner and fuel, to analytically study the characteristics of MRT instability in a finite slab using the ideal MHD model.[15] Later, authors also studied the effect of magnetic shear on the MRT instability and the feedthrough of outer surface ripples originated from MRT instability on inner surface perturbations.[16,17] Recently, authors studied the MRT instability in cylindrical shells analytically and designed special magnetic field to mitigate MRT instability.[18–20] Above theoretical studies are mainly based on incompressible assumption. However, it is known that the temperature of liner plasmas is relatively low during the liner implosion, because the liner is very heavy in the MagLIF concept compared to the large radius wire-array Z-pinch. In this case, the compressibility may play an important role on MRT instability, deserving careful investigation.

In this paper, the MRT instability in compressible three-region plasmas is theoretically investigated. The dispersion relation of MRT instability is derived using a slab model in Section 2, and the characteristics of MRT instability in (x,y) plane is discussed in Section 3 . The summary is given in Section 4.

*Project supported by the National Natural Science Foundation of China (Grant Nos. 11475027, 11274051, 11105017, and 11275030) and the National Basic Research Program of China (Grants No. 2013CB834100).

†Corresponding author. E-mail: xiao_delong@iapcm.ac.cn

© 2017 Chinese Physical Society and IOP Publishing Ltd

2. Derivation of dispersion relation

In this paper, we use a three-region slab model to analyze MRT instability in MagLIF as shown in Fig. 1. Region I represents the vacuum, region II represents the metal liner, and region III represents the fuel. $x = 0$ is the axis of the liner, and $x = r_{\rm i}$, $x = r_{\rm o}$ are the position of the inner and outer surfaces of the liner, respectively.

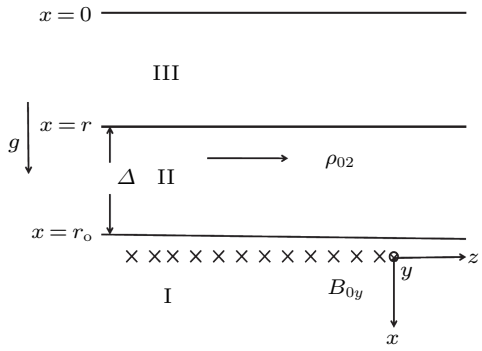


Fig. 1. MRT model with two interfaces at $x = r_{\rm i}$ and at $x = r_{\rm o}$.

In the rest frame of the outer interface, the ideal MHD equations can be written as follows:

$$\rho\left(\frac{\partial}{\partial t}+\boldsymbol{v}\cdot\boldsymbol{\nabla}\right)\boldsymbol{v}=-\boldsymbol{\nabla}p+\boldsymbol{J}\times\boldsymbol{B}+\rho g\boldsymbol{x}, \tag{1}$$

$$\frac{\partial\rho}{\partial t}+\boldsymbol{\nabla}\cdot(\rho\boldsymbol{v})=0, \tag{2}$$

$$\frac{\partial\boldsymbol{B}}{\partial t}=\boldsymbol{\nabla}\times(\boldsymbol{v}\times\boldsymbol{B}), \tag{3}$$

$$\boldsymbol{\nabla}\times\boldsymbol{B}=\mu_0\boldsymbol{J}, \tag{4}$$

$$\left(\frac{\partial}{\partial t}+\boldsymbol{v}\cdot\boldsymbol{\nabla}\right)(p\rho^{-\tilde{\gamma}})=0, \tag{5}$$

where ρ and $\boldsymbol{v}$ are the mass density and the velocity, respectively; p and $\boldsymbol{J}$ are the plasma pressure and the current density; $\boldsymbol{B}$ is the magnetic field, g is the equivalent gravity in the x direction; $\boldsymbol{x}$ is the unit vector, and μ_0 is the free space permeability. $\tilde{\gamma}$ is the adiabatic coefficient. The pressure, velocity, and magnetic field can be written in the perturbation form

$$\begin{aligned}
p &= p_0(x)+p_1(x)\,{\rm e}^{(\gamma t-{\rm i}k_y y-{\rm i}k_z z)},\\
\boldsymbol{v} &= \boldsymbol{v}_0+\boldsymbol{v}_1\equiv\gamma\boldsymbol{\xi}_1=\gamma[\xi_{1x}(x),\xi_{1y}(x),\xi_{1z}(x)]\,{\rm e}^{(\gamma t-{\rm i}k_y y-{\rm i}k_z z)},\\
\boldsymbol{B} &= \boldsymbol{B}_0(x)+\boldsymbol{B}_1\\
&= \boldsymbol{B}_0(x)+[B_{1x}(x),B_{1y}(x),B_{1z}(x)]\,{\rm e}^{(\gamma t-{\rm i}k_y y-{\rm i}k_z z)},
\end{aligned} \tag{6}$$

where quantities with a subscript 0 and quantities with a subscript 1 are the equilibrium quantities and the small signal quantities, respectively. By linearizing Eqs. (1)–(5) and $\boldsymbol{\nabla}\cdot\boldsymbol{B}=0$, the perturbation quantities can be given by

$$\gamma\rho_0 v_{1\perp}={\rm i}\boldsymbol{k}P+\frac{1}{\mu_0}\left[-{\rm i}(\boldsymbol{k}\cdot\boldsymbol{B}_0)B_{1\perp}+B_{1x}\frac{\partial\boldsymbol{B}_0}{\partial x}\right], \tag{7}$$

$$\gamma\rho_0 v_{1x}=-\frac{\partial P}{\partial x}+\frac{1}{\mu_0}[-{\rm i}(\boldsymbol{k}\cdot\boldsymbol{B}_0)B_{1x}]+\rho_{1g}, \tag{8}$$

$$\gamma\rho_1+v_{1x}\frac{\partial\rho_0}{\partial x}+\rho_0\frac{\partial v_{1x}}{\partial x}-\rho_0({\rm i}\boldsymbol{k}\cdot\boldsymbol{v}_{1\perp})=0, \tag{9}$$

$$\gamma B_{1x}=-{\rm i}\boldsymbol{k}\cdot\boldsymbol{B}_0 v_{1x}, \tag{10}$$

$${\rm i}(\boldsymbol{k}\cdot\boldsymbol{B}_{1\perp})=\frac{\partial B_{1x}}{\partial x}, \tag{11}$$

$$\gamma p_1+v_{1x}\frac{\partial p_0}{\partial x}+c_{\rm s}^2\rho_0\frac{\partial v_{1x}}{\partial x}+c_{\rm s}^2\rho_0(-{\rm i}\boldsymbol{k}\cdot\boldsymbol{v}_{1\perp})=0, \tag{12}$$

where $P=p_1+\frac{\boldsymbol{B}_0\cdot\boldsymbol{B}_1}{\mu_0}$. $\boldsymbol{k}$ is the wave vector. $c_{\rm s}=\frac{\partial p}{\partial\rho_0}=\frac{\tilde{\gamma}p_0}{\rho_0}$ is the acoustic velocity. The equilibrium condition is written as $-\boldsymbol{\nabla}(p_0+\frac{B_0^2}{2\mu_0})+\rho_0 g=0$. In this paper, we only study the MRT instability in (x,y) plane as shown in Fig. 1, so we set $\boldsymbol{k}=k_y\hat{y}=k\hat{y}$, $\boldsymbol{B}_0=B_{0y}\hat{y}=B_0\hat{y}$, and $B_{0z}=0$. By eliminating p_1, ρ_1, B_{1x}, B_{1y}, v_{1y} using Eqs. (7)–(12), we can obtain an eigenvalue equation of perturbation displacement as follows:

$$\begin{aligned}
&\frac{\partial}{\partial x}\left\{\left[\frac{\gamma^2k^2c_{\rm s}^2}{\gamma^2+k^2c_{\rm s}^2}\rho_0+\frac{(kB_0)^2}{\mu_0}\right]\frac{\partial\xi_{1x}}{\partial x}\right\}\\
&=k^2\left\{\left[\gamma^2-\frac{k^2g^2}{\gamma^2+k^2c_{\rm s}^2}\right]\rho_0\right.\\
&\quad\left.+\frac{k^2c_{\rm s}^2g}{\gamma^2+k^2c_{\rm s}^2}\frac{\partial\rho_0}{\partial x}+\frac{(kB_0)^2}{\mu_0}\right\}\xi_{1x}.
\end{aligned} \tag{13}$$

Considering that the plasmas of region I and region III are incompressible ($c_{\rm s}\to\infty$), the density ρ_0 and the magnetic field B_0 are constant and uniform, then equation (13) can be written as

$$\frac{\partial^2\xi_{1x}}{\partial x^2}-k^2\xi_{1x}=0. \tag{14}$$

Designating $\xi_{\rm i}=\xi_{1x}(r_{\rm i})$ and $\xi_{\rm o}=\xi_{1x}(r_{\rm o})$, the solution to Eq. (14) is given by

$$\xi_{1x}(x)=\xi_{\rm i}\frac{\sinh(kx)}{\sinh(kr_{\rm i})},\quad 0<x<r_{\rm i}, \tag{15}$$

$$\xi_{1x}(x)=\xi_{\rm o}\frac{{\rm e}^{-kx}}{{\rm e}^{-kr_{\rm o}}},\quad x>r_{\rm o}. \tag{16}$$

Considering that the plasma of region II is compressible and the magnetic field B_0 is constant and uniform, and $\frac{\partial\rho_0}{\partial x}=\frac{\tilde{\gamma}\rho_{02}g}{c_{\rm s}^2}$, equation (13) can be written as

$$\begin{aligned}
&\left[1+\frac{\gamma^2+k^2c_{\rm s}^2}{\gamma^2k^2c_{\rm s}^2}\frac{(kB_{02})^2}{\mu_0\rho_{02}}\right]\frac{\partial^2\xi_{1x}}{\partial x^2}+\frac{\tilde{\gamma}g}{c_{\rm s}^2}\frac{\partial\xi_{1x}}{\partial x}\\
&-\left[\frac{\gamma^2+k^2c_{\rm s}^2}{c_{\rm s}^2}+\frac{k^2g^2}{\gamma^2c_{\rm s}^2}(\tilde{\gamma}-1)\right.\\
&\left.+\frac{\gamma^2+k^2c_{\rm s}^2}{\gamma^2c_{\rm s}^2}\frac{(kB_{02})^2}{\mu_0\rho_{02}}\right]\xi_{1x}=0,
\end{aligned} \tag{17}$$

where ρ_{02} is the density of the liner. The solution of the above equation is $\xi_{1x}=A\exp(\lambda_1 x)+B\exp(\lambda_2 x)$, where

$$\lambda_{1,2}=\frac{-\frac{\tilde{\gamma}g}{c_{\rm s}^2}\pm\sqrt{\frac{\tilde{\gamma}^2g^2}{c_{\rm s}^4}+4\left[1+\frac{\gamma^2+k^2c_{\rm s}^2}{\gamma^2k^2c_{\rm s}^2}\frac{(kB_{02})^2}{\mu_0\rho_{02}}\right]\left[\frac{\gamma^2+k^2c_{\rm s}^2}{c_{\rm s}^2}+\frac{k^2g^2}{\gamma^2c_{\rm s}^2}(\tilde{\gamma}-1)+\frac{\gamma^2+k^2c_{\rm s}^2}{\gamma^2c_{\rm s}^2}\frac{(kB_{02})^2}{\mu_0\rho_{02}}\right]}}{2\left[1+\frac{\gamma^2+k^2c_{\rm s}^2}{\gamma^2k^2c_{\rm s}^2}\frac{(kB_{02})^2}{\mu_0\rho_{02}}\right]}. \tag{18}$$

Because the perturbation displacement is continuous at the interface, the values of A and B can be obtained from Eqs. (15)–(18) as follows:

$$A=\frac{-\xi_{\rm i}\,{\rm e}^{\lambda_2\Delta}+\xi_{\rm o}}{{\rm e}^{\lambda_1 r_{\rm i}}F_\Delta}, \tag{19}$$

$$B=\frac{\xi_{\rm i}\,{\rm e}^{\lambda_1\Delta}-\xi_{\rm o}}{{\rm e}^{\lambda_2 r_{\rm i}}F_\Delta}, \tag{20}$$

where $F_\Delta={\rm e}^{\lambda_1\Delta}-{\rm e}^{\lambda 2\Delta}$ and $\Delta=r_{\rm o}-r_{\rm i}$ is the liner thickness. Then we integrate Eq. (13) across the outer surface to yield

$$\frac{\xi_{\rm i}}{\xi_{\rm o}}=\frac{-\frac{k^4c_{\rm s}^2g\rho_{02}}{\gamma^2+k^2c_{\rm s}^2}+k\frac{(kB_{01})^2}{\mu_0}}{\left[\rho_{02}\frac{\gamma^2k^2c_{\rm s}^2}{\gamma^2+k^2c_{\rm s}^2}+\frac{(kB_{02})^2}{\mu_0}\right]\frac{\lambda_1-\lambda_2}{F_\Delta}\,{\rm e}^{(\lambda_1+\lambda_2)\Delta}}+\frac{\lambda_1\,{\rm e}^{\lambda_1\Delta}-\lambda_2\,{\rm e}^{\lambda_2\Delta}}{(\lambda_1-\lambda_2)\,{\rm e}^{(\lambda_1+\lambda_2)\Delta}}=F. \tag{21}$$

Similarly, using the above method at the inner surface, we can obtain

$$\frac{\xi_{\rm o}}{\xi_{\rm i}}=\frac{\frac{k^4c_{\rm s}^2g\rho_{02}}{\gamma^2+k^2c_{\rm s}^2}+k\frac{(kB_{03})^2\coth kr_{\rm i}}{\mu_0}}{\left[\rho_{02}\frac{\gamma^2k^2c_{\rm s}^2}{\gamma^2+k^2c_{\rm s}^2}+\frac{(kB_{02})^2}{\mu_0}\right]\frac{\lambda_1-\lambda_2}{F_\Delta}}+\frac{\lambda_1\,{\rm e}^{\lambda_2\Delta}-\lambda_2\,{\rm e}^{\lambda_1\Delta}}{(\lambda_1-\lambda_2)}=\frac{1}{F}, \tag{22}$$

where B_{01}, B_{02}, and B_{03} are the magnetic field of region I, region II, and region III, respectively. F is the feedthrough factor, which is defined as the ratio of the perturbation displacement at the two interface, can be used to describe the feedthrough effect between the perturbations of the two liner surfaces. Employing Eqs. (21) and (22), we can obtain a dispersion relation of the growth rate γ of MRT instability as

$$\left\{\frac{-\frac{k^4c_{\rm s}^2g\rho_{02}}{\gamma^2+k^2c_{\rm s}^2}+k\frac{(kB_{01})^2}{\mu_0}}{\left[\rho_{02}\frac{\gamma^2k^2c_{\rm s}^2}{\gamma^2+k^2c_{\rm s}^2}+\frac{(kB_{02})^2}{\mu_0}\right]\frac{\lambda_1-\lambda_2}{F_\Delta}\,{\rm e}^{(\lambda_1+\lambda_2)\Delta}}+\frac{\lambda_1\,{\rm e}^{\lambda_1\Delta}-\lambda_2\,{\rm e}^{\lambda_2\Delta}}{(\lambda_1-\lambda_2)\,{\rm e}^{(\lambda_1+\lambda_2)\Delta}}\right\}\times\left\{\frac{\frac{k^4c_{\rm s}^2g\rho_{02}}{\gamma^2+k^2c_{\rm s}^2}+k\frac{(kB_{03})^2\coth kr_{\rm i}}{\mu_0}}{\left[\rho_{02}\frac{\gamma^2k^2c_{\rm s}^2}{\gamma^2+k^2c_{\rm s}^2}+\frac{(kB_{02})^2}{\mu_0}\right]\frac{\lambda_1-\lambda_2}{F_\Delta}}+\frac{\lambda_1\,{\rm e}^{\lambda_2\Delta}-\lambda_2\,{\rm e}^{\lambda_1\Delta}}{(\lambda_1-\lambda_2)}\right\}=1. \tag{23}$$

The analytic solution of Eq. (23) is hardly obtained, and the growth rate can be numerically calculated. However, we can simplify Eq. (23) and get the analytic growth rate in several limiting situations. Firstly, in the incompressible condition $c_{\rm s}\to\infty$, $\lambda_{1,2}=\pm k$, equation (23) is then reduced to

$$\left[\gamma^2+\frac{(kB_{02})^2}{\mu_0\rho_{02}}\right]^2+\left[\gamma^2+\frac{(kB_{02})^2}{\mu_0\rho_{02}}\right]\times\left[\frac{(kB_{01})^2}{\mu_0\rho_{02}}+\frac{(kB_{03})^2}{\mu_0\rho_{02}}\coth kr_{\rm i}\right]\coth k\Delta+\left[\frac{(kB_{01})^2}{\mu_0\rho_{02}}-kg\right]\left[\frac{(kB_{03})^2}{\mu_0\rho_{02}}\coth kr_{\rm i}+kg\right]=0, \tag{24}$$

which is consistent to that in Ref. [21]. Setting $r_{\rm i}\to\infty$, $\Delta=\infty$, and $B_{01}=0$, equation (24) will be reduced to $\gamma^2=k|g|-\frac{(kB_{02})^2}{\mu_0\rho_0}-\frac{(kB_{03})^2}{\mu_0\rho_0}$, which is the classical form in two-region model. In the case of zero magnetic field, it is further reduced to $\gamma^2=k|g|$.

Secondly, in the case of zero magnetic field and large liner thickness, equation (23) will also be reduced to the dispersion relation as that in Ref. [22], which will be discussed in the following section.

3. MRT instability in (x,y) plane

In this paper, we choose the typical liner quantities on the Z experiments as examples to analyze the MRT instability.[2,23,24] The liner material is beryllium and its density is $\rho_{02}=1.85\ {\rm g/cm^3}$. The liner thickness is $\Delta=0.540$ mm.

For MRT instability developing in (x,y) plane, which corresponds to (r,θ) plane in cylindrical liner implosions, we can set $k_z=0$. In this case, only azimuthal magnetic field B_{0y} will affect the development of MRT instability. In MagLIF, typical implosion distance is several millimeters and the implosion time is several tens of nanoseconds, causing a high acceleration to 10^{-4} cm/ns^2. Figure 2 describes the variations of the growth rate γ with the gravity g in compressible and incompressible situations for different magnetic field in the case of $c_{\rm s}=5\times10^3$. It is shown that the growth rate in compressible assumption is approximately the same as that in incompressible assumption when the magnetic field is zero. However, in the presence of magnetic field the growth rate is obviously decreased in compressible condition compared to that in incompressible condition.

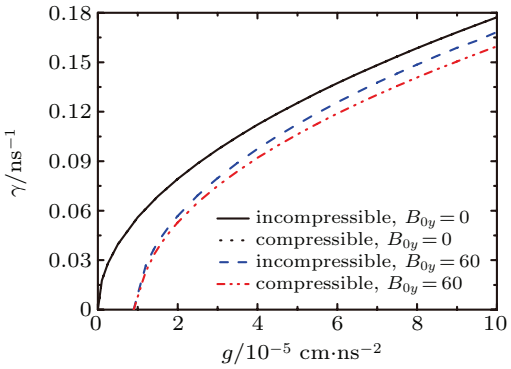


Fig. 2. (color online) Variations of the growth rate γ with the gravity g.

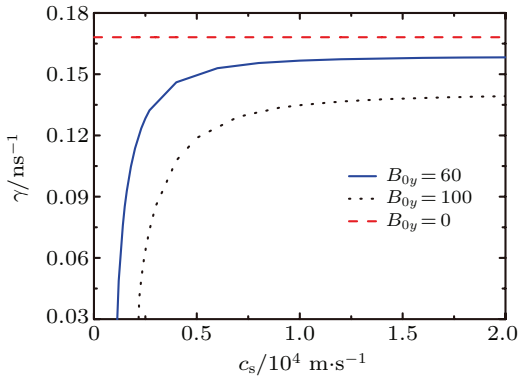


Fig. 3. (color online) Variations of the growth rate γ with the acoustic velocity c_s in different magnetic field.

In order to explain this phenomenon, we firstly discuss the situation of zero magnetic field and large liner thickness Δ. In this case, the growth rate can be simplified as

$$\gamma^2 = k^2 g/\lambda_1. \tag{25}$$

If the acoustic velocity c_s is very large, λ_1 is reduced to k, thus giving the growth rate $\gamma^2 = kg$. If $c_s \ll 1$, λ_1 can be given by

$$\begin{aligned}\lambda_1 &= -\frac{\tilde{\gamma} g}{2c_s^2} + \sqrt{\frac{\gamma^2 + k^2 c_s^2}{c_s^2} + \frac{k^2 g^2}{\gamma^2 c_s^2}(\tilde{\gamma}-1) + \frac{\tilde{\gamma}^2 g^2}{4c_s^4}} \\ &\approx \frac{1}{\tilde{\gamma}}\frac{\gamma^2}{g} + \frac{\tilde{\gamma}-1}{\tilde{\gamma}}\frac{k^2 g}{\gamma^2}.\end{aligned} \tag{26}$$

Equations (25) and (26) will also yield the same growth rate $\gamma^2 = kg$ as that in very large c_s. That is to say, compressibility will not obviously change the MRT development in the case of zero magnetic field. However, when the magnetic field is present and is frozen in the plasma, it will also be compressed as the plasma is compressed. Hence, it can provide stronger restoring force to mitigate MRT instability when the plasma is compressible. In order to further investigate the compressibility effect on MRT instability, the variations of the growth rate γ with the acoustic velocity c_s are plotted in Fig. 3. It is obviously shown that the growth rate is nearly independent of c_s in the case of zero magnetic field. The growth rate increases with c_s when the magnetic field is 60 T or 100 T. When c_s is very large, the growth rate will approach the classical $\gamma^2 = kg - \frac{(kB_0)^2}{\mu_0 \rho_0}$, as shown in Fig. 3.

It is noted that the growth rate is remarkably dependent on the perturbation wavelength. Figure 4 shows the variations of growth rate γ with the perturbation wavelength λ_y with magnetic field $B_{0y} = 0$ and 60 T. It is shown that the growth rate decreases monotonically with λ_y when $B_{0y} = 0$ T. However, the growth rate reaches a maximal value when $B_{0y} = 60$ T at $\lambda_y = 41$ μm. Furthermore, the presence of magnetic field has a stronger effect on mitigating smaller wavelength perturbations.

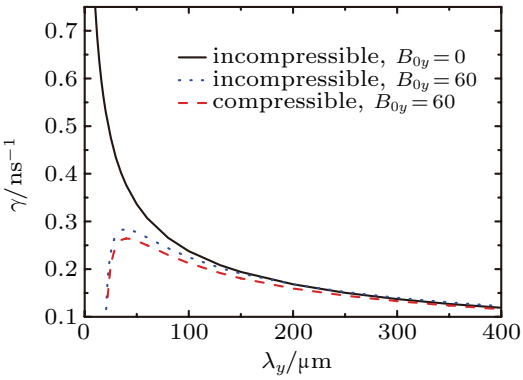


Fig. 4. (color online) Variations of the growth rate γ with perturbation wavelength λ_y with magnetic field $B_{0y} = 0$ and 60 T.

Clearly, large wavelength perturbations are more serious for MRT instability. The variations of growth rate with B_{0y} in the case of $\lambda_y = 400$ μm and $\lambda_y = 800$ μm are compared in compressible and incompressible condition in Fig. 5 for $g = 10^{-4}$ cm/ns^2. It is shown that as the magnetic field increases, the growth rate is remarkably decreased and even be reduced to zero whether in compressible condition or in incompressible condition. It is also shown that the longer the perturbation wavelength is, the higher the B_{0y} is needed to decrease the growth rate to zero. For the case of large perturbation wavelength 400 μm, when B_{0y} exceeds 364 T, the growth rate is decreased to zero. For the smaller wavelength perturbation, it is more easy to decrease the growth rate to zero. As is known that during the liner implosion, B_{0y} will increase to over 1000 T. In this case, the growth rate of MRT instability for almost all perturbation wavelengths can be decreased to zero. Therefore, the development of MRT instability in (x, y) plane, or in (r, θ) plane in cylindrical liner implosions can be nearly completely mitigated. However, in (x, z) plane the axial magnetic field is just several tens of Tesla. Hence, the growth rate in (x, z) plane cannot be reduced to zero, though largely mitigated by the axial magnetic field.

The MRT instability developing initially on the outer surface may feed to the inner surface. The feedthrough factor F measures this effect of perturbation at one interface on the

other interface.[16,21] The feedthrough can provide significant seeding at inner interface when the implosion is slowed down or Richtmyer–Meshkov (RM) instability is developed. The feedthrough is only related to the perturbation wavelength and the thickness when the magnetic field is zero with a simple form $F = \exp(-k\Delta)$. Figure 6 shows that the feedthrough factor F increases with perturbation wavelength λ_y, where the gravity $g = 10^{-4}$ cm/ns^2. We also find that the feedthrough is decreased in compressible condition compared to that in incompressible condition when the magnetic field is not zero.

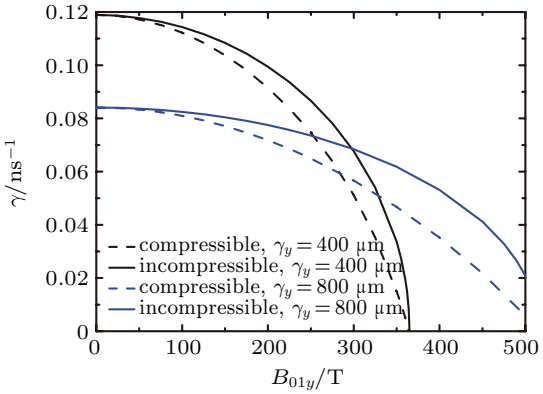


Fig. 5. (color online) Variations of the growth rate γ with the magnetic field B_{0y} with $\lambda_y = 400$ μm and $\lambda_y = 800$ μm.

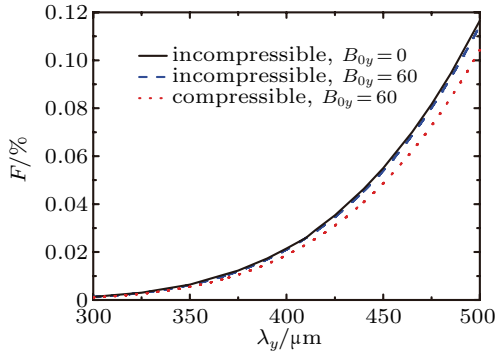


Fig. 6. (color online) Variations of the feedthrough factor F with the perturbation wavelength λ_y with magnetic field $B_{0y} = 0$ and 60 T.

4. Summary

In this paper the characteristics of MRT instability of liner plasmas in MagLIF is theoretically investigated. A three-region slab model, based on ideal MHD equations, is used to derive the dispersion relation of MRT instability. The effect of compressibility on the development of MRT instability is specially examined. It is shown that in the case of zero magnetic field, the growth rate in compressible assumption is approximately the same as that in incompressible assumption. However, the growth rate of MRT instability in compressible condition is generally lower than that in incompressible condition, because the magnetic field frozen in the plasma can provide stronger restoring force when the plasma is compressible. When the acoustic velocity c_s is small, this effect is more remarkable. When c_s is large, the growth rate will approach that in incompressible condition. It is also shown that in the case of zero magnetic field, the growth rate monotonically decreases with perturbation wavelength. The presence of magnetic field can remarkably reduce the growth rate specially for short-wavelength perturbations. The growth rate of MRT instability in the (x,y) plane may be decreased to zero because the magnetic field can be increased to over 1000 T and completely mitigate the perturbations during liner implosions.

We also discuss the feedthrough of MRT instability of outer liner surface on inner surface perturbation. It is shown that in the case of zero magnetic field, the feedthrough factor depends on the perturbation wavelength and liner thickness, independent of compressibility or incompressibility condition. However, when the magnetic field is not zero, the feedthrough factor in compressible condition is generally much lower than that in incompressible condition, because the feedthrough factor also depends on the growth rate of MRT instability, which varies evidently between compressible and incompressible assumptions.

Acknowledgement

The authors would like to acknowledge professor Li Ding for useful suggestions to derive the accurate dispersion relation of MRT instability in this paper.

References

[1] Slutz S A, Herrmann M C, Vesey R A, Sefkow A B, Sinars D B, Rovang C R, Peterson K J and Cuneo M E 2010 *Phys. Plasmas* **17** 056303
[2] Awe T J, McBride R D, Jennings C A, Lamppa D C, Martin M R, Rovang D C, Sinars D B, Slutz S A, Owen A C, Tomlinson K, Gomez M R, Hansen S B, Herrmann M C, McKenney J L, Robertson G K, Rochau G A, Savage M E, Schroen D G and Stygar W A 2014 *Phys. Plasmas* **21** 056303
[3] Slutz S A and Vesey R A 2012 *Phys. Rve. Lett.* **108** 025003
[4] Sinars D B, Slutz S A, Herrmann M C, McBride R D, Cuneo M E, Jennings C A, CHittenden J P, Velikovich A L, Peterson K J, Vesey R A, Nakhleh C, Waisman E M, Blue B E, Killebrew K, Schroen D, Tomlinson K, Edens A D, Lopez M R, Smith C, Shores J, Bigman V, Bennett G R, Atherton B W, Savage M, Stygar W A, Leifeste G T and Porter J L 2011 *Phys. Plasmas* **18** 056301
[5] Ryutov D D, Cuneo M E, Herrmann M C, Sinars D B and Slutz S A 2012 *Phys. Plasmas* **19** 062706
[6] Zhang Y and Ding Ning 2005 *Acta Phys. Sin.* **55** 2333 (in Chinese)
[7] Ding Ning, Zhang Y, Xiao D L, Wu J M, Dai Z H, Yin L, Gao Z M, Sun S K, Xue C, Ning C, Shu X J and W J G 2016 *Matter and Radiation at Extremes* **1** 135
[8] Awe T J, McBride R D, Jennings C A, Lamppa D C, Martin M R, Rovang D C, Slutz S A, Cuneo M E, Owen A C, Sinars D B, Tomlinson K, Gomez M R, Hansen S B, Herrmann M C, McKenney J L, Nakhleh C, Robertson G K, Rochau G A, Savage M E, Schroen D G and Stygar W A 2013 *Phys. Rev. Lett.* **111** 235005
[9] Chandrasekhar S 1961 *Hydrodynamic and Hydromagnetic Stability* (London: Oxford University) Chap. VIII, p. 429
[10] Harris E G 1962 *Phys. Fluids* **5** 1057
[11] Yang B L, Wang L F, Ye W H and Xue C 2011 *Phys. Plasmas* **18** 072111
[12] Zhang W L, Wu Z W and Li D 2005 *Phys. Plasmas* **12** 042106
[13] Bud'ko A B, Felber F S, Kleev A I, Liberman M A and Velikovich A L 1989 *Phys. Fluids B* **1** 598
[14] Bellan P M 2006 *Fundamentals of Plasma Physics* (Cambrige: Cambrige University Press)

[15] Lau Y Y, Zier J C, Rittersdorf I M, Weis M R and Gilgenbach R M 2011 *Phys. Rev. E* **83** 066405

[16] Zhang P, Lau Y Y, Rittersdorf I M, Weis M R, Gilgenbach R M, Chalenski D and Slutz S A 2012 *Phys. Plasmas* **19** 022703

[17] Amendt P, Colvin J D, Ramshaw J D, Robey H F and Landen O L 2003 *Phys. Plasmas* **10** 820

[18] Ryutov D D and Dorf M A 2014 *Phys. Plasmas* **21** 112704

[19] Velikovich A L and Schmit P F 2015 *Phys. Plasmas* **22** 122711

[20] Schmit P F, Velikovich A L, McBride R D and Robertson G K 2016 *Phys. Rev. Lett.* **117** 205001

[21] Weis M R, Zhang P, Lau Y Y, Rittersdorf I M, Zier J C, Gilgenbach R M, Hess M H and Peterson K J 2014 *Phys. Plasmas* **21** 122708

[22] Livescu D 2004 *Phys. Fluids* **16** 118

[23] Gomez M R, Slutz S A, Sefkow A B, Sinars D B, Hahn K D, Hansen S B, Harding E C, Knapp P F, Schmit P F, Jennings C A, Geissel T J, Rovang D C, Chandler G A, Cooper G W, Cuneo M E, HaveyThompson A J, Herrmann M C, Hess M H, Johns O, Lamppa D C, Martin M R, McBride R D, Peterson K J, Porter J L, Robertson G K, Rochau G A, Ruiz C L, Savage M E, Smith I C, Stygar W A and Vesey R A 2014 *Phys. Rev. Lett.* **113** 155003

[24] Sinars D B, Slutz S A, Herrmann M C, McBride R D, Cuneo M E, Peterson K J, Vesey R A, Nakhleh C, Blue B E, Killebrew K, Schroen D, Tomlinson K, Edens A D, Lopez M R, Smith I C, Shores J, Bigman V, Bennett G R, Atherton B W, Savage M, Stygar W A, Leifeste G T and Porter J L 2010 *Phys. Rev. Lett.* **105** 185001